Available online at www.sciencedirect.com
ScienceDirect
Surface & Coatings Technology 202 (2008) 2194–2201
SURFACE & COATINGS TECHNOLOGY
www.elsevier.com/locate/surfcoat

Multilayer silica-methacrylate hybrid coatings prepared by sol–gel on stainless steel 316L: Electrochemical evaluation

Damián A. López [a], Nataly C. Rosero-Navarro [b], Josefina Ballarre [a], Alicia Durán [b], Mario Aparicio [b], Silvia Ceré [a,*]

[a] *INTEMA, Universidad Nacional del Mar del Plata-CONICET, Juan B. Justo 4302, B7608FDQ, Mar del Plata, Argentina*
[b] *Instituto de Cerámica y Vidrio (CSIC), Campus de Cantoblanco, 28049 Madrid, Spain*

Received 17 July 2007; accepted in revised form 10 September 2007
Available online 18 September 2007

Abstract

AISI 316L stainless steel is a biocompatible alloy used in prosthetic devices for many years. However this alloy tends to suffer localized corrosion and needs external fixation to hard tissues. This work describes the development of a coating system of two layers with complementary properties. The inner layer is prepared using TEOS and MTES that has already shown good anticorrosion properties. The top layer is a new hybrid organic–inorganic coating prepared with TEOS, 3-methacryloxypropyl trimethoxysilane (MPS), and 2-hydroxyethyl methacrylate (HEMA). The properties of this sol let to produce a thick and porous coating formed by two interpenetrating (organic and inorganic) networks. This coating could be an excellent container for the later aggregate of bioactive particles as the following step in a future work based on its high thickness, plasticity and open structure to allow the electrolyte access to induce the formation of hydroxyapatite. The coating is electrochemically characterised in simulated body fluid at 37 °C after 1, 10 and 30 days of immersion by means of assays as electrochemical impedance spectroscopy (EIS) and polarization curves. The dual coating seems to join the best properties of the individual ones in time: their thickness restrict the passage of potentially toxic ions to the body fluid, the breakdown potential (Eb) remains high and far from the corrosion potential (Ecorr) and the film presents the open structure of the outer layer that allows the entrance of the electrolyte to react with the particles when added to the sol meanwhile the inner layer maintain its corrosion protective features.

PACS: 81.20.Fw-; 82.45.Bb-; 87.68.+Z
Keywords: Stainless steel; Coatings; Orthopaedics alloys; Sol–gel; Corrosion

1. Introduction

AISI 316L stainless steel is regarded as a biocompatible material. It has been used in the fabrication of prosthetic devises for many years, mostly in applications where the implant is temporary, although it is also used as permanent implants in many developing countries. However, this alloy tends to suffer localised corrosion and releases significant quantities of iron ions to the neighbouring tissues leading to risk of local tumours and mechanical failure of the implant [1–7]. The use of AISI 316L for permanent prosthesis would be very advantageous since the cost is much reduced respecting to the other usual Ti or Co–Cr alloys. In those cases, the application of coatings that reduce the release of the potentially toxic ions to the human body and increase the corrosion resistance would be necessary. In one hand these coatings should be biocompatible and able to resist the same stresses than the alloy; in the other hand they could be functionalized with bioactive particles in order to avoid the cementing of the prosthesis by promoting natural fixation to hard and soft tissues.

Coatings produced by the sol gel procedure have been proposed as an adequate system to make protective [8–14] as well as bioactive [15–19] coatings.

* Corresponding author. INTEMA, Corrosion Division, UNMdP, Juan B. Justo 4302, B7608FDQ, Mar del Plata, Argentina. Tel.: +54 223 4816600; fax: +54 223 4810046.
E-mail address: smcere@fi.mdp.edu.ar (S. Ceré).

0257-8972/$ - see front matter © 2007 Elsevier B.V. All rights reserved.
doi:10.1016/j.surfcoat.2007.09.007

It has been demonstrated that inorganic and hybrid SiO_2 coatings obtained from tetraethylorthosilicate (TEOS) and methyltriethoxysilane (MTES) as precursors in acidic catalysts, improve the corrosion behaviour of the AISI 316L stainless steel in biological environments [10]. These coatings were applied as mono and multilayer by a multistep method. XPS analysis of inorganic and hybrid SiO_2 coatings on steel substrates showed that TEOS as only precursor allows certain extent of Fe diffusion, but the hybrid coatings prepared from MTES/TEOS limited the diffusion of iron [20]. When glass or glass ceramic particles in the system $CaO–SiO_2–P_2O_5$ are added to the hybrid system, *in vitro* bioactivity is observed although the protective effectiveness of the coating diminishes in time due to the entrance of the electrolyte into pores or small fissures [21]. The use of a double layer, one devoted to act as corrosion and diffusion barrier, and the other to contain glass and glass-ceramic particles demonstrated an important bioactivation on *in-vitro* and *in-vivo* tests and prolonged corrosion resistance [22,23]. However, the high density of the quasi-inorganic top coating delays the bioactive response.

The objective of this work is the development of a coating system of two layers with complementary properties. The inner layer is prepared using TEOS and MTES that has already shown good anticorrosion properties and very low iron diffusion. The top layer is a new hybrid organic–inorganic coating prepared from TEOS, 3-methacryloxypropyl trimethoxysilane (MPS), and 2-hydroxyethyl methacrylate (HEMA). The synthesis and structural characterization of the precursor sol have been previously reported [24]. The properties of this sol allow to produce thick and porous coatings formed by two interpenetrating (organic and inorganic) networks. These coatings could be excellent containers for the later aggregate of bioactive particles, as the following step in a future work based on its high thickness, plasticity and open structure to allow the electrolyte access to induce the formation of hydroxyapatite shortcoming the bioactive response. This new double-layer coating should act as a Fe diffusion as well as corrosion barrier to accomplish the requirements of minimum Fe release and corrosion protection of metals used in orthopedics.

2. Experimental procedure

2.1. Preparation and characterization of sols

Two different sol–gel solutions have been synthesized to prepare multilayer coatings on the substrates. The first was a hybrid organic–inorganic sol prepared with a silicon alkoxide, tetraethylorthosilicate (TEOS), and an alkylalkoxide, methyltriethoxysilane (MTES), with a methyl group attached to the silicon atom that provide a slight organic behaviour. Both precursors were purchased to ABCR and used without further purification. This sol was prepared firstly mixing absolute ethanol, TEOS and MTES (molar ratio TEOS/MTES = 40/60), adding HNO_3 0.1 N (molar ratio water/TEOS + MTES = 1.7) and acetic acid (molar ratio water/acetic acid = 7) under stirring at 40 °C for three hours.

The second sol is also a hybrid organic–inorganic one with a higher organic content in order to produce thicker coatings. TEOS, 3-methacryloxypropyl trimethoxysilane (MPS) from ABCR, and 2-hydroxyethyl methacrylate (HEMA) from ALDRICH were used as precursors. HEMA is a monomer able to generate an organic structure through opening of double bonds. MPS is an organically modified alkoxide that improves the bond at molecular level of both, organic and inorganic networks. This compound can polymerize through hydrolysis and condensation reactions of three methoxy

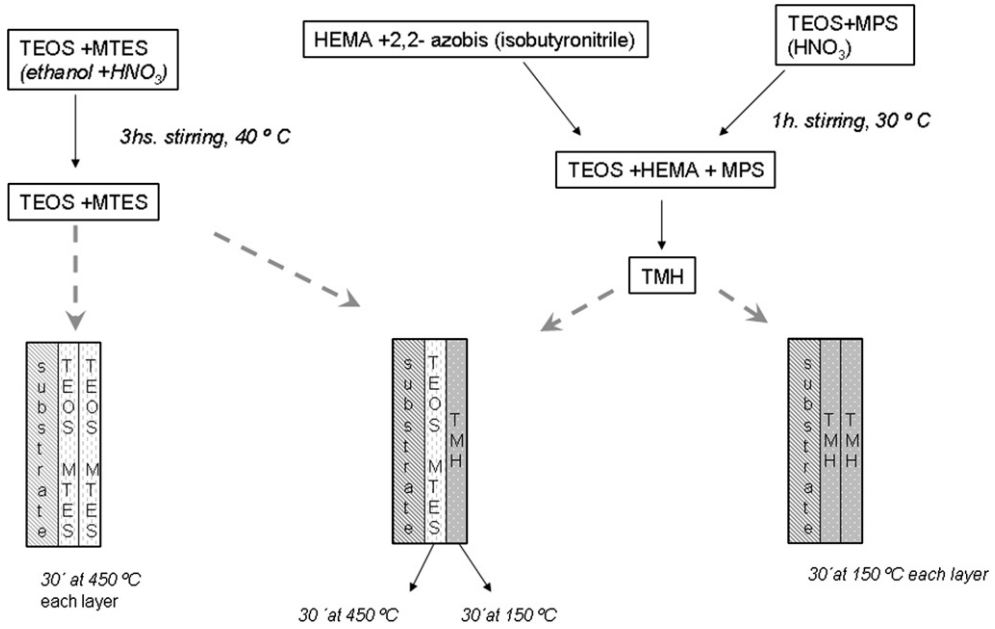

Fig. 1. Scheme of coating deposition.

groups to produce a Si–O–Si network connecting with the inorganic structure from TEOS, and also has a vinyl group that promotes organic polymerization together with the structure from HEMA. The result is a hybrid structure with two (organic and inorganic) interpenetrating networks attached by chemical bonds. The sol has a molar composition of TEOS/HEMA/MPS = 60/30/10, and was prepared by mixing two solutions. The first solution was synthesized by mixing isopropanol, TEOS, MPS and HNO_3 0.1 N (molar ratio water/TEOS + MPS = 1.9) stirring at 30 °C for one hour. The second solution was prepared by stirring at room temperature for 30 min isopropanol, HEMA and 2,2′-azobis(isobutyronitrile) (AIBN) from Fluka in 1 mol% with respect of MPS + HEMA as initiator of the free-radical copolymerization. Both solutions were mixed and stirred at room temperature for another 30 min. Finally, the sol was cured at 65 °C in order to promote the organic polymerization of HEMA and MPS. The viscosity of both sols was measured using a rheometer RS50 (Haake, Germany).

2.2. Substrates and coatings

Coatings were deposited on soda-lime glass slides and stainless steel (316L) sheets. Glass (2.5×7 cm^2) and 316L samples (5×10 cm^2) were degreased, hand washed with distilled water, and rinsed in ethanol.

Coatings prepared with TEOS-MTES sol were obtained at room temperature by dip-coating using a withdrawal rate of 30 cm min^{-1}, dried at room temperature for 30 min, and heat treated for 30 min at 450 °C in electric furnace. The sol TEOS-MPS-HEMA (TMH) was also used to prepare coatings on both substrates using a withdrawal rate of 25 cm min^{-1}, dried at room temperature for 30 min, and heat treated for 30 min at 150 °C. Two-layer coatings with a TEOS-MTES layer directly on the substrate and a TMH layer on the previous layer were prepared using the same procedure shown above. Fig. 1 shows a scheme of coating deposition.

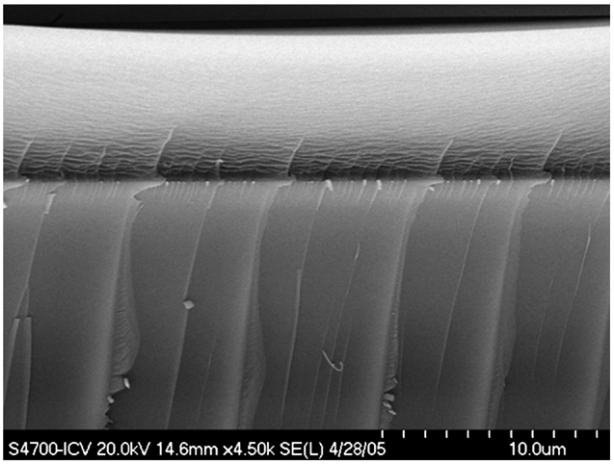

Fig. 2. SEM micrograph of a cross section of a multilayer coating over a glass substrate.

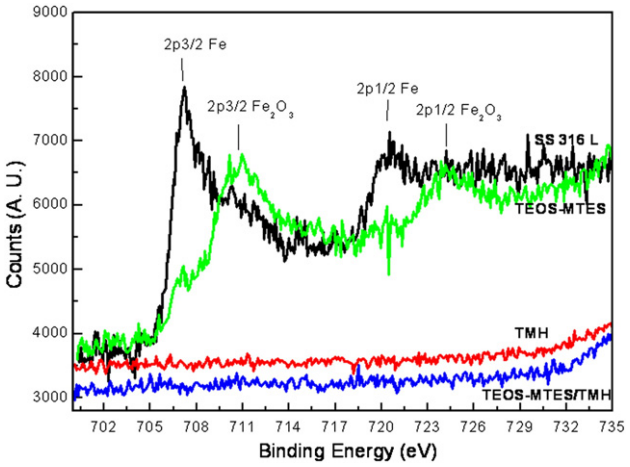

Fig. 3. High resolution XPS scans for Fe 2p with 120 s of sputtering with Ar^+ in the samples immersed in SBF for 30 days.

The coating homogeneity and adherence was evaluated by scanning electron microscopy (HITACHI S-4700 field emission) after fracture of the substrate. Coating thickness was measured on glass substrates after densification by using a profilometer (Talystep, Taylor-Hobson, UK) on a scratch. The thickness was also studied by SEM using a cross section of the coating.

X-ray photoelectron spectroscopy (XPS) spectra were taken using a commercial VG ESCA 3000 system. The base pressure in the experimental chamber was in the low 10^{-9} mbar range. The spectra were collected using Mg Kα (1253.6 eV) radiation and the overall energy resolution was about 0.8 eV. Survey spectra were recorded for the samples in the 0–1100 eV kinetic energy range by 1 eV steps. High resolution scans with 0.1 eV steps were conducted over Fe 2p, Cr 2p and Ni 2p. In all the cases surface charging effects were compensated by referencing the binding energy (BE) to the C 1s line of residual carbon set at 284.6 eV BE [25]. Sputtering of the sample surface was performed with an argon ion gun under an accelerating voltage

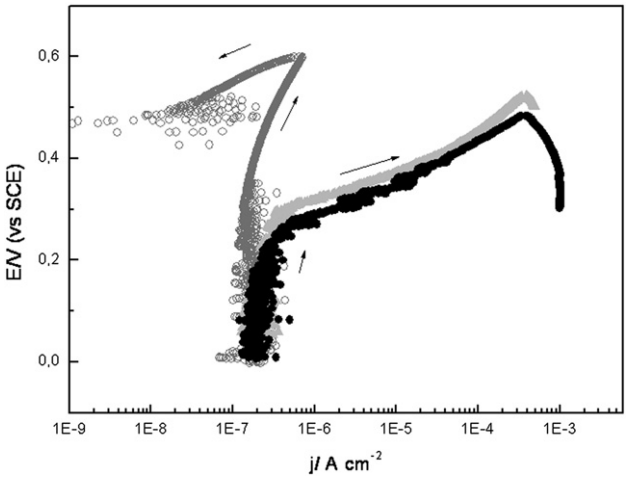

Fig. 4. Potentiodynamic polarization curve for the TMH coating after 1(●) and 30 (○) days of immersion in SBF and their comparison with the bare alloy (●). $v = 0.002$ Vs^{-1}.

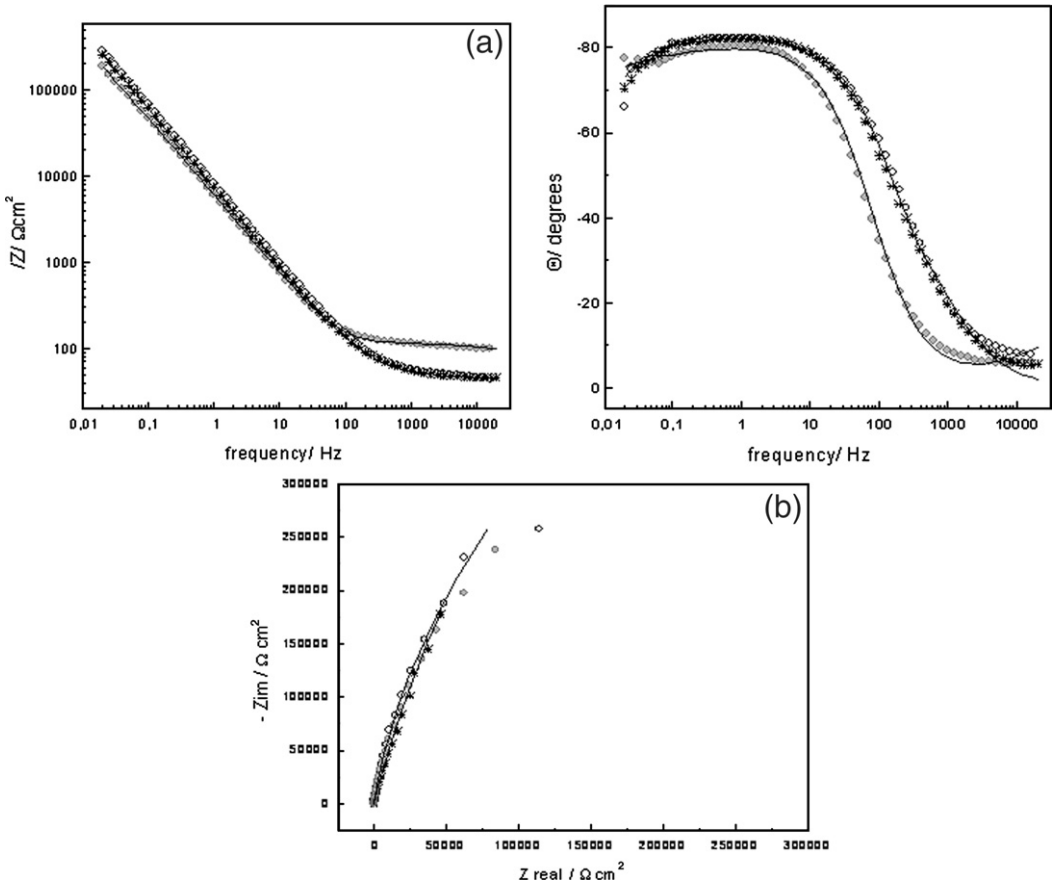

Fig. 5. Bode (a) and Nyquist (b) plots for the TMH coating after 1(◍), 10 (*) and 30 (○) days of immersion in SBF. Solid lines represent the modelled results.

of 3 kV. All the samples were measured after 120 s of Ar^+ sputtering.

2.3. Electrochemical assays

Electrochemical assays were conducted in a Solartron 1280B electrochemical unit. A conventional three electrode cell was used with a saturated calomel electrode (SCE; Radiometer) as reference electrode and a platinum wire as counter electrode. All electrochemical assays were held after stabilization of Ecorr for at least 24 h. Potentiodynamic polarization curves were conducted from the corrosion potential (Ecorr) to 1.1 V and backwards, or up to a maximum current density of 1 mA cm^{-2}, at a sweep rate of 0.002 V s^{-1}. Electrochemical spectroscopy impedance (EIS) test were registered at the E_{corr} with an amplitude of 0.005 V rms sweeping frequencies from 20,000 to 0.01 Hz. Impedance data fitting was performed using Zplot software [26]. Electrochemical test were conducted after 1 and 30 days of immersion in SBF for Potentiodynamic polarization and 1, 10 and 30 days of immersion in SBF for EIS assays.

3. Results and discussion

Both sols were transparent, colourless the TEOS-MTES sol and slightly yellowish the TMH sol. Viscosities were 1.8 and 3.9 cP respectively for the above named sols. The difference in the measured viscosity is a consequence of the higher viscosity of HEMA and the organic polymerization promoted during the synthesis [24].

Both coatings appear homogeneous and crack-free. The average thickness obtained using the profilometer has been

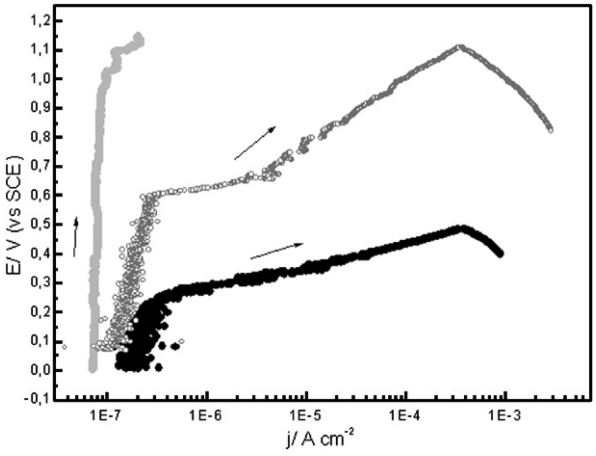

Fig. 6. Potentiodynamic polarization curve for the TEOS-MTES coating after 1 (◍) and 30 (○) days of immersion in SBF and their comparison with the bare alloy (●). v=0.002 Vs^{-1}.

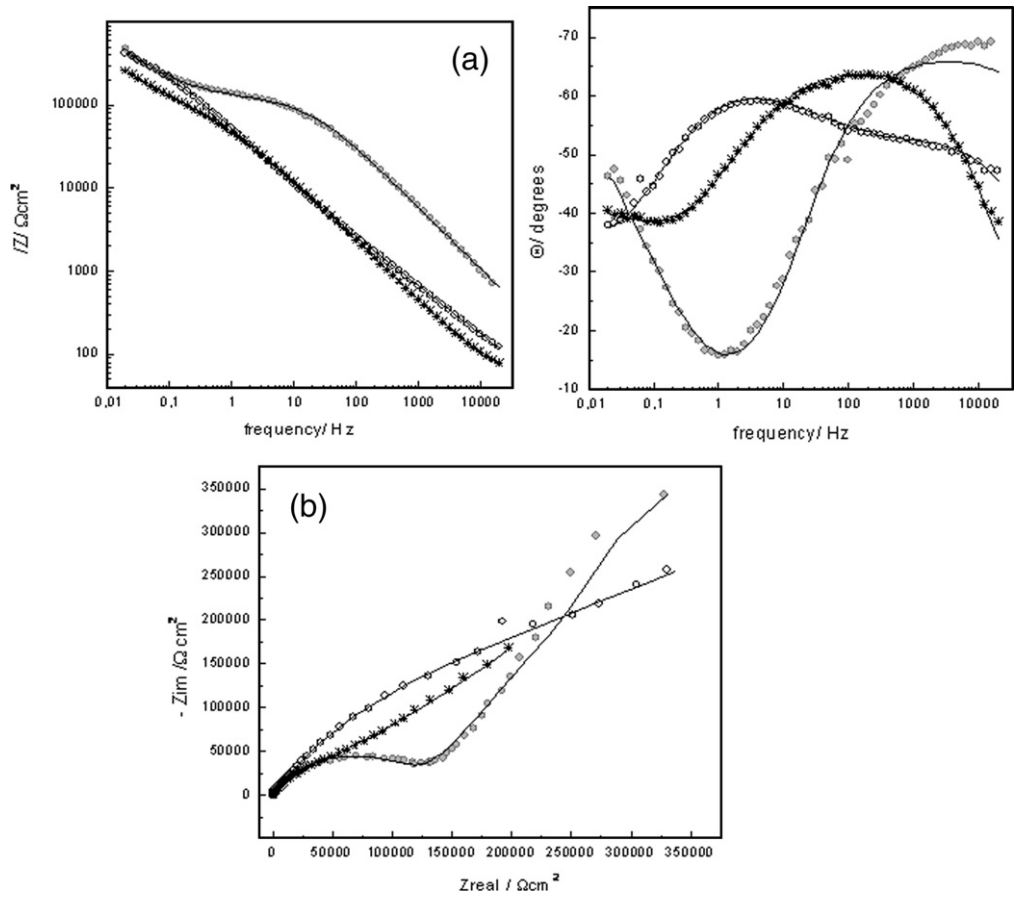

Fig. 7. Bode (a) and Nyquist (b) plots for the TEOS-MTES coating after 1(●), 10 (*) and 30 (○) days of immersion in SBF. Solid lines represent the modelled results.

1.5 and 3.8 μm for the TEOS-MTES and TMH coating, respectively.

In previous work, typical mechanic and elastic properties of these hybrid coatings, as well as creep behaviour have been studied [27]. Young modulus (E) and hardness (H) are the first insight to know the scratch behaviour and adhesive response, and for these coatings (TEOS-MTES, TMH and TEOS-MTES/TMH) the values are 6.5, 3 and 3.8 GPa for *E*, and 0.92, 0.16 and 0.22 GPa for *H* respectively. The nano-scratch technique is the most used one for analyze adhesion of thin films to hard substrates. The system of TEOS-MTES/TMH coatings seems to be able to resist punctual loads of more than 75 mN and the surface recover is almost complete with no delamination and little plastic deformation [28].

Fig. 2 shows a SEM micrograph of a cross section of a multilayer coating over a glass substrate. The coating looks homogeneous, crack-free and adhered to the substrate. The residual stresses observed are the consequence of sample preparation by direct fracture of the substrate.

Fig. 3 presents the high resolution XPS scans for Fe 2p with 120 s of sputtering with Ar^+ in the samples immersed in the studied conditions for 30 days. It can be observed that Fe is only detected in the TEOS-MTES hybrid coating. XPS scans do not show Fe in samples coated with TMH or double-layer coatings. The bigger thickness of these coatings compared with TEOS-MTES ones limits the Fe diffusion to the surface, demonstrating the barrier effect of these coatings against ion diffusion.

Fig. 4 shows the Potentiodynamic polarization curve for the TMH coating after 1 and 30 days of immersion in SBF. After

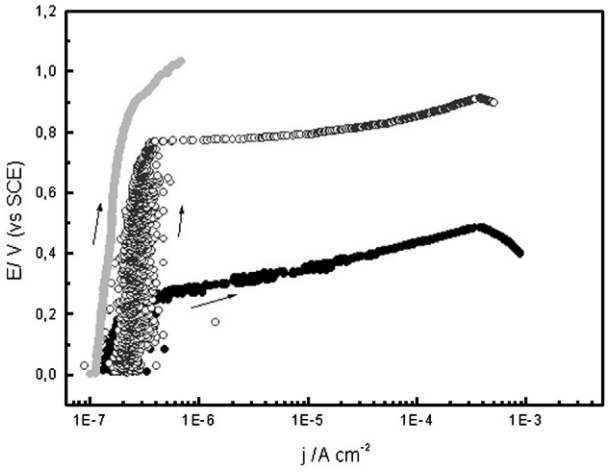

Fig. 8. Potentiodynamic polarization curve for the TEOS MTES+TMH coating after 1(●) and 30 (○) days of immersion in SBF and their comparison with the bare alloy (●). v=0.002 Vs^{-1}.

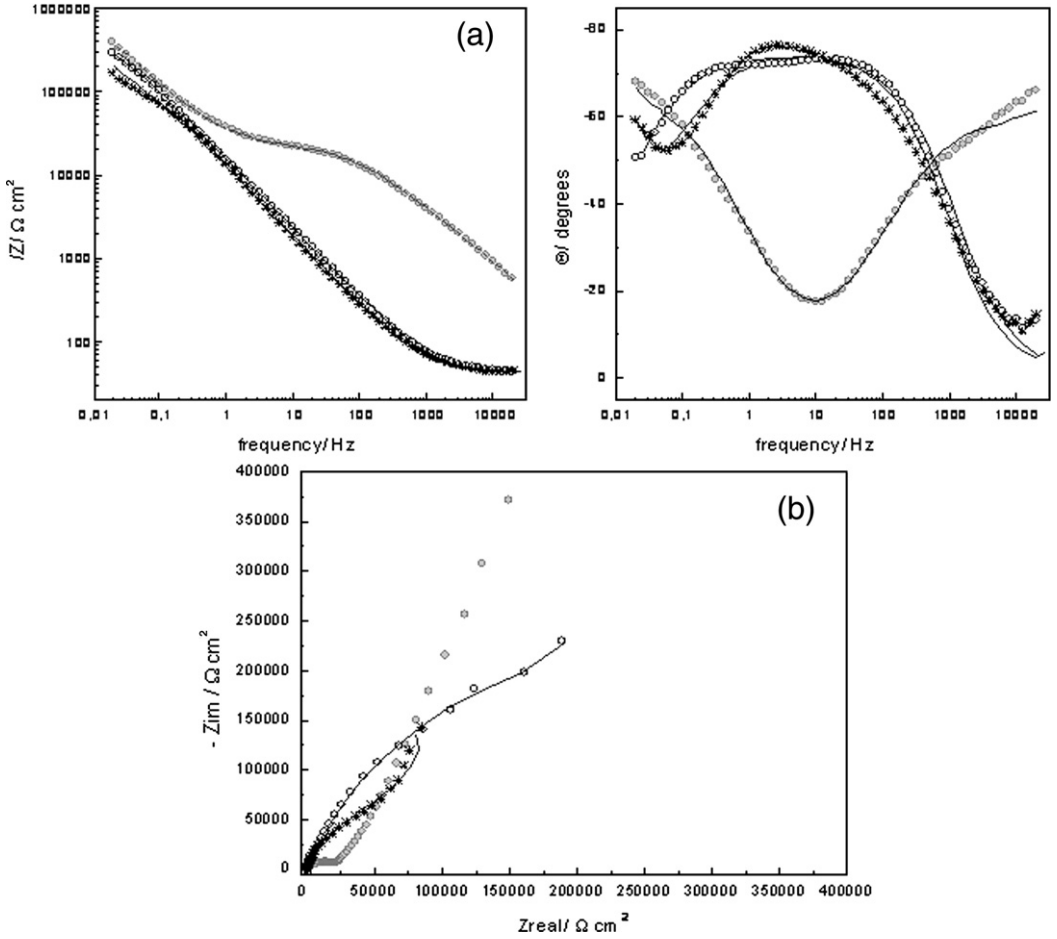

Fig. 9. Bode (a) and Nyquist (b) plots for the TEOS-MTES + TMH coating after 1(●, 10 (*) and 30 (○) days of immersion in SBF. Solid lines represent the modelled results.

1 day the response is nearly the same than that of the bare steel but after 30 days of immersion an enhance in the breakdown potential (Eb) is observed for the coated sample, not showing localised corrosion in the range of potentials under study. EIS tests on TMH coatings do not reveal remarkable differences among the coated samples and the bare steel (Fig. 5).The phase angle vs frequency data do not indicate a clear maxima. A small increase in the phase angle up to 80° with frequency was found, indicating a non conducting behaviour at frequencies up to 50 Hz. At higher frequencies some conductivity is shown, as it can be seen from the decrease in the phase angle. A shift to higher angles in the high frequency range is observed after 30 days of immersion in SBF indicating that the film after 30 days has somehow less conductivity paths than the one after 1 d of immersion.

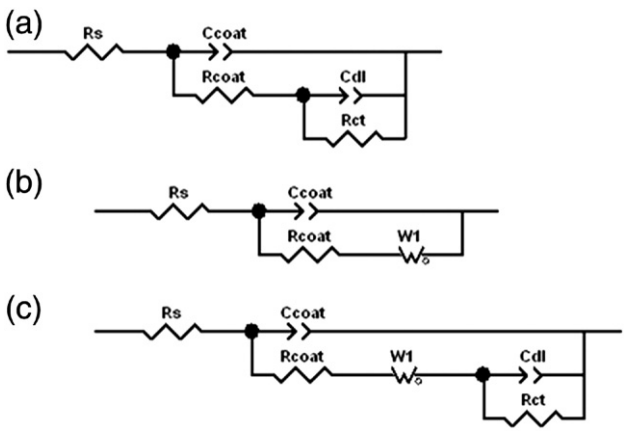

Fig. 10. Equivalent electric circuits employed to model the impedance data a) TMH coating 1, 10 and 30 d of immersion in SBF. b) TEOS-MTES after 1 and 10 d and TEOS-MTES/TMH after 1, 10 and 30 d of immersion in SBF. c) TEOS-MTES after 30 d of immersion in SBF.

Fig. 6 shows the Potentiodynamic polarization curve for the coatings obtained with the TEOS-MTES hybrid coating. It can be observed that, in agreement with previous works [20,21,29], TEOS-MTES coatings act as an effective barrier to the electrolyte entrance in the coating after 1 d of immersion in SBF showing less passivity current density and a shift of the Eb of 0.85 V respect to the bare alloy. After 30 d of immersion the film slightly deteriorates but it always remains with less passive current density and higher Eb than the bare material. Fig. 7 shows the EIS plots in Bode and Nyquist representation of the samples coated with TEOS-MTES coatings. After 1 d immersion, the coating shows two time constants. In the low

Table 1

	$R_s/\Omega\ cm^2$	$R_{coat}/\Omega\ cm^2$	$C_{coat}/\Omega^{-1}\ cm^{-2}\ s^n$	n_c	$R_{DO}/\Omega\ cm^2$	T/s	n	$C_{dl}/\Omega^{-1}\ cm^{-2}\ s^n$	n_d	$R_{dl}/\Omega\ cm^2$
TMH										
1 d	45.6	52.7	$1.25\ 10^{-5}$	0.81	–	–	–	$1.96\ 10^{-5}$	0.95	$2.66\ 10^{6}$
10 d	43.7	96.47	$1.43\ 10^{-5}$	0.91	–	–	–	$1.28\ 10^{-5}$	0.92	$1.59\ 10^{6}$
30 d	45.6	122.7	$1.76\ 10^{-5}$	0.88	–	–	–	$4.64\ 10^{-5}$	1	$2.99\ 10^{6}$
TEOS-MTES										
1 d	43	$1.28\ 10^{5}$	$2.31\ 10^{-7}$	0.75	$1.40\ 10^{6}$	55.95	0.65	–	–	–
10 d	42	$5.93\ 10^{4}$	$3.59\ 10^{-7}$	0.74	$1.43\ 10^{6}$	60.67	0.61	–	–	–
30 d	44	$4.81\ 10^{3}$	$4.22\ 10^{-6}$	0.66	$6.17\ 10^{5}$	41.5	0.76	$1.01\ 10^{-6}$	0.75	$3.17\ 10^{5}$
TEOS-MTES/TMH										
1 d	45	$2.38\ 10^{4}$	$5.26\ 10^{-7}$	0.69	$1.56\ 10^{6}$	50.27	0.73	–	–	–
10 d	44	$1.71\ 10^{5}$	$1.60\ 10^{-5}$	0.84	$1.51\ 10^{6}$	81.7	0.89	–	–	–
30 d	43.86	$6.01\ 10^{5}$	$1.37\ 10^{-5}$	0.83	$9.78\ 10^{5}$	77.3	0.94	–	–	–

frequency region a diffusive behaviour is observed. After 30 d of immersion, two time constants are still observed but a change in the mechanism is evidenced by the drop of the angle *vs* frequency plot in the low frequency region. This could be interpreted as a defective coating involving porous penetration of the electrolyte [30].

Fig. 8 shows the potentiodynamic polarization curve for the coating that combines both hybrid systems. After 1 d of immersion the performance is very similar to that presented for the TEOS-MTES system. After 30 d of immersion the current density around the corrosion potential is analogous to the other studied systems but the Eb is shifted positive respect to both systems, reaching 0.8 V. EIS diagrams, in the Bode and Nyquist format, are shown in Fig. 9 for the system TEOS-MTES/TMH. After 1 d of immersion a diffusive behaviour is observed similar to that of TEOS-MTES coating system. Accordingly, after 30 d of immersion two time constants are more clearly defined, showing some deleterious effect on the coating with time.

Impedance spectra were fitted using the equivalent circuits shown in Fig. 10. Fitted parameters are shown in Table 1 and a solid line in Figs. 5, 7 and 9 shows the goodness of the fitting. Constant phase elements instead of capacitances were used in the work when phase angle capacitor was different from −90°. Accordingly, Ccoat and Cdl represent the pseudocapacitance of the coating and double layer respectively and n is a coefficient associated to the system homogeneity (being 1 for an ideal capacitor). Rs, Rcoat and Rdl, represent the solution, coating and double layer resistance respectively. The Warburg impedance is used to model increasing ionic conductivity due to corrosion processes occurring inside the pores and the increasing diffusivity into them. If the material is thin, low frequencies will penetrate the entire thickness, creating a finite length Warburg element (Eq. (1)) [26].

$$Z_w = \frac{R_{DO}}{(jT\omega)^n}\tanh(jT\omega)^n \quad (1)$$

In this equation, R_{DO} is associated with solid phase diffusion and T is related to diffusion coefficient and pore length.

It can be observed that the total resistance is similar for all samples at all immersion times. However Rcoat, related to the resistance in the coating pores, is very low for the TMH coating indicating that the electrolyte penetrates into the pores and takes contact with the base alloy. The open structure of the coating as well as its hydrophilic nature (due to the daggling OH groups in their structure) [24] assists the entrance of the electrolyte into the film. The almost constant value of Ccoat in TMH coatings with the immersion time also reflects the access of electrolyte into the pores of the coating. Ccoat can be defined by Eq. (2).

$$\mathrm{Ccoat} = \varepsilon\varepsilon_0 A/d \quad (2)$$

In this equation, ε is the dielectric constant of the coating, ε_0 the free space permittivity, A the testing area and d the coating thickness. The water uptake in coatings can be monitored by the increase of Ccoat due to the increase of ε because the dielectric constant of water is around 80, higher than those of organic and inorganic coatings (in the range of 5–10). However, the water uptake in the pores of the TMH produces an increase in the coating thickness likely compensating the value of the dielectric constant of water and thus leading to a near constant value of Ccoat.

The fitting parameters for the TEOS-MTES coating system and the TEOS-MTES/TMH coating system after 1 day of immersion are similar. Although the thickness of the dual coating is bigger than that of TEOS-MTES coating, the open structure of the TMH outside layer allows the entrance of the electrolyte. Thus, the inner near-inorganic layer is the only that acts as a barrier for the electrolyte and in turn offers some corrosion protection, presenting a high diffusion resistance in their structure. After 30 days, some detrimental effect is observed in the coating systems. Rcoat diminishes for the TEOS-MTES and slightly increases for the other two coating systems, besides an increase in Ccoat is observed linked to water uptake or an area effect related to an increase of defects in the coating. Ccoat increases more noticeably for the dual coating TEOS-MTES/TMH related to TEOS-MTES one.

The double-layer coating developed has shown an excellent combination of properties: very low iron diffusion, anticorrosion properties and enhancement of electrolyte access to the top layer

that will lead to a higher bioactivity and a quicker *in-vitro* and *in-vivo* response.

4. Conclusions

Two-layer hybrid sol–gel coatings on stainless steel AISI 316L were obtained using TEOS and MTES and TEOS, MPS, and HEMA (TMH) with the aim of obtaining coatings with complementary properties. The TMH coating presents an open structure with interconnected pores that permits the access of the electrolyte into the coating. This, in turn could favoured the dissolution of bioactive particles that could be added to the sol and are an essential step to induce the hidroxyapatite deposition on the particles.

The doble-layer coating seems to join the best properties of the individual coatings with time: their thickness restricts the diffusion of potentially toxic ions to the body fluid and the Eb remains high and far from the E_{corr}, showing that it is acting as corrosion barrier.

Acknowledgements

The authors would like to thanks National Research Council of Argentina (Conicet), Spanish project MAT2006-4375 and Dr. Wido Schreiner of the University of Parana (Brasil) Secyt-Capes Cooperation Project 174/04.

References

[1] G. Wintere, J. Biomed. Mater. Res. Symp. 5 (1974) 11.
[2] Metals handbook, Ninth Edition, Corrosion, vol. 13, ASM International, Metals Park, Ohio, 1987, p. 1324.
[3] Y. Okazaki, E. Gotoh, T. Manabe, K. Kobayashi, Biomaterials 25 (2004) 5913.
[4] J. Bullen, H. Rogers, P. Spalding, C. Ward, FEMS Immunol. Med. Microbiol. 43 (2005) 325.
[5] D.B. McGregor, R.A. Baan, C. Partensky, J.M. Rice, J.D. Wilbourm, Eur. J. Cancer 36 (2000) 307.
[6] J.A. Disegi, L. Eschbach, Injury, Int. J. Care Injured 31 (2000) S–D2-6.
[7] D.A. López, A. Durán, S. Ceré, J. Mater. Sci., Mater. Med., (in press).
[8] O. de Sanctis, L. Gómez, N. Pellegri, C. Parodi, A. Marajofsky, A. Durán, J. Non-Cryst. Solids 121 (1990) 338.
[9] J.J. de Damborenea, N. Pellegrini, O. de Sanctis, A. Durán, J. Sol–gel Sci. Technol. 4 (1995) 239.
[10] P. Galliano, J.J. de Damborenea, M.J. Pascual, A. Durán, J. Sol–gel Sci. Technol. 13 (1998) 723.
[11] B. Naderi Zand, M. Mahdavian, Electrochim. Acta 52 (2007) 6438.
[12] Y. Castro, B. Ferrari, R. Moreno, A. Durán, Surf. Coat. Technol. 191 (2005) 228.
[13] T.P. Chou, C. Chandrasekaran, S.J. Limmer, S. Seraji, Y. Wu, M.J. Forbess, C. Nguyen, G.Z. Cao, J. Non-Cryst. Solids 290 (2001) 153.
[14] J.-M. Yeh, C-J. Weng, W-J. Liao, Y-W. Mau, Surf. Coat. Technol. 201 (2006) 1788.
[15] M.J. Filiaggi, R.M. Pilliar, 21th Annual Meeting of Society for Biomaterials, 1995.
[16] J. Gallardo, R. Moreno, P. Galliano, A. Durán, J. Sol–gel Sci. Technol. 19 (2000) 107.
[17] M. Metikos-Hukovic, E. Tkalcec, A. Kwokal, J. Piljac, Surf. Coat. Tech. 165 (2003) 40.
[18] L. Gan, R. Pilliar, Biomaterials 25 (2004) 5303.
[19] K. Cheng, S. Zhang, W. Weng, Thin Solid Films 515 (2006) 135.
[20] J. Gallardo, P. Galliano, A. Durán, J. Sol–gel Sci. Technol. 21 (2001) 65.
[21] C. Garcia, S. Ceré, A. Durán, J. Non-Cryst. Solids 348 (2004) 218.
[22] A. Durán, A. Conde, A. Gomez Coedo, T. Dorado, C. Garcia, S. Ceré, J. Mater. Chem. 14 (2004) 2282.
[23] J. Ballarre, J.C. Orellano, C. Bordenave, P. Galliano, S. Ceré, J. Non-Cryst. Solids 304 (2002) 278.
[24] S.A. Pellice, R.J.J. Williams, I. Sobrados, J. Sanz, Y. Castro, M. Aparicio, A. Durán, J. Mater. Chem. 16 (2006) 3318.
[25] F. Moulder, in: W.F. Stickle, P.E. Sobol, K.D. Bomben (Eds.), Handbook of X-Ray Photoelectron Spectroscopy, Physical Electronics, Inc., Eden Praire, Minnesota 55344, USA, 1995.
[26] Zplot for Windows, Electrochem. Impedance Software Operating Manual, Part 1, Scribner Ass. Inc., Southern Pines, NC, 1998.
[27] J. Ballarre, D.A. López, A.L. Cavalieri, Thin Solid Films (2007), doi:10.1016/j.tsf.2007.07.186.
[28] J. Ballarre, D.A. López, A.L. Cavalieri, Wear (in press).
[29] L.E. Amato, D.A. López, P.G. Galliano, S. Ceré, Mater. Lett. 59 (2005) 2026.
[30] M. Kendig, J. Scully, Corrosion 46 (1990) 22.